Chemical Engineering Science 245 (2021) 116847

Contents lists available at ScienceDirect

Chemical Engineering Science

journal homepage: www.elsevier.com/locate/ces

Mechanism and kinetics of the aerobic oxidation of benzyl alcohol to benzaldehyde catalyzed by cobalt porphyrin in a membrane microchannel reactor

Qi Han [a], Xian-Tai Zhou [a,*], Xiao-Qi He [d], Hong-Bing Ji [b,c,*]

[a] Fine Chemical Industry Research Institute, School of Chemical Engineering and Technology, Sun Yat-sen University, Zhuhai 519082, China
[b] Fine Chemical Industry Research Institute, School of Chemistry, Sun Yat -sen University, Guangzhou 510275, China
[c] School of Chemical Engineering, Guangdong University of Petrochemical Technology, Maoming 525000, China
[d] Huizhou Research Institute, Sun Yat-sen University, Huizhou 516081, China

HIGHLIGHTS

- Benzyl alcohol oxidation was achieved in a membrane microchannel reactor.
- Mechanism involving free radical and high-valence species was demonstrated.
- Benzyl alcohol oxidation exhibited the features of Michaelis–Menten kinetics.

GRAPHICAL ABSTRACT

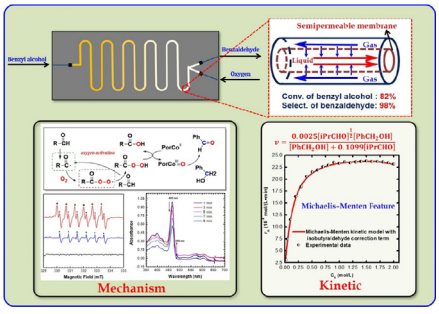

ARTICLE INFO

Article history:
Received 7 January 2021
Received in revised form 23 May 2021
Accepted 3 June 2021
Available online 5 June 2021

Keywords:
Benzyl alcohol
Oxidation
Membrane microchannel reactor
Mechanism
Kinetics
Cobalt porphyrins

ABSTRACT

The highly efficient selective aerobic oxidation of benzyl alcohol to benzaldehyde catalyzed by cobalt porphyrin was achieved in a membrane microchannel reactor. The efficiency of benzyl alcohol oxidation was remarkably improved in the micro-structured chemical system, achieving a conversion and benzaldehyde selectivity of 82% and 98%, respectively, in 6.5 min. The classification and transfer of free radicals, as well as the oxygen-transfer mechanism, were determined by *in situ* EPR (electron paramagnetic resonance) and *in situ* UV–visible spectroscopy. Further kinetic studies revealed that the oxidation of benzyl alcohol follows the Michaelis–Menten kinetics, with K_m = 0.133 mol/L.A mathematic kinetic model was proposed, and the kinetic model fitted the experimental data well. The mathematical model can predict the reaction process at a wide range of benzyl alcohol concentrations, which is beneficial for the process optimization and reactor design.

1. Introduction

Selective oxidation of benzyl alcohol to benzaldehyde is a crucial process (Mallat and Baiker, 2004; Zhang et al., 2012; Sankar et al., 2020; Groppo et al., 2018) because the product benzaldehyde is immensely valuable in organic synthesis (Vinod, et al., 2011; Xu, 1996; Torbina et al., 2018). Considerable advances have been made in the field, involving the use of stochiometric oxidants such as TBHP (*tert*-butyl hydroperoxide) (Sarmah et al., 2010; Frija et al., 2017), hydrogen peroxide (Guo and Li, 2007; Jing et al., 2013; Cang et al., 2015), etc. (Yadav and Krishnan, 1999; Xiao et al., 2019; Di Somma et al., 2017; Cerdan et al., 2019) leading to environmental problems and high costs. From the viewpoints of the

* Corresponding authors at: Fine Chemical Industry Research Institute, School of Chemistry, Sun Yat -sen University, Guangzhou 510275, China (H.-B. Ji).
E-mail addresses: zhouxtai@mail.sysu.edu.cn (X.-T. Zhou), jihb@mail.sysu.edu.cn (H.-B. Ji).

https://doi.org/10.1016/j.ces.2021.116847
0009-2509/

environment and cost, molecular oxygen is the most desirable oxidant for catalytic oxidation (Ji et al., 2003; Liu et al., 2018; Li et al., 2017). The activization of dioxygen, the key step of aerobic oxidation of alcohol (Ma et al., 2019), alkene (Eisenberg et al., 2018; Denekamp et al., 2018) and ester (Zhang et al., 2020) had been solved to a certain extent in the presence of metals particles on active supports. Hence, various catalytic systems such as ruthenium (Al-Rifai et al., 2016; Ji et al., 2007; Han et al., 2020), cobalt (Yang et al., 2016; Wang et al., 2018), manganese (Meng et al., 2013; Fu et al., 2017), etc. (Satrio and Doraiswamy, 2002) have been developed for the selective aerobic oxidation of benzyl alcohol.

Although immense progress for the selective aerobic oxidation of benzyl alcohol has been reported, most of the catalytic oxidation procedures have been conducted in a bubble column on the laboratory scale (Liu et al., 2017; Kobayashi et al., 2006; Olenin et al., 2018). In a bubble column reactor, the catalytic efficiency is adversely affected by the gas-liquid mass transfer, which limits its industrial implementation (Ide et al., 2018; Zhao et al., 2018). Hence, the aerobic oxidation of benzyl alcohol in the continuous flow mode is significant for the large-scale preparation of benzaldehyde (Wu and Wang, 2003; Rebrov et al., 2012; Vina-Gonzalez et al., 2019).

In recent years, several researchers have focused on the use of a microchannel due to its wide applications in the chemical industry, such as in organic synthesis (Schonfeld et al., 2004; Hu et al., 2018; Zeng et al., 2018; Tabakova, 2019), nanomaterial preparation (Othman et al., 2015; Sharaf et al., 2019; Zhao et al., 2013), and industrial catalytic oxidation (Bawornruttanaboonya et al., 2017; Venkateswaran et al., 2019; Liu et al., 2019; Dai et al., 2019; Snytnikov et al., 2010). A plug-flow model is utilized to describe the fluid flow in the micro-channel with a diameter of only 10–1000 μm. The hydromechanical characteristics of the fluid in the microchannel reactor change remarkably compared with those in the bubble column reactor. This special structure exhibits unique benefits: The reaction time and temperature can be precisely controlled; prompt mixing can be realized in the presence of a micro-mixed element; and uniform mass and heat transfer can be achieved in the microchannel (Shen et al., 2015; Zhang et al., 2021).

Among these approaches, membrane reactors are attracting immense attention due to their well-defined contact interface between the gas and liquid phases. A mesh-supported Teflon AF-2400 membrane has been used for the oxidation of benzyl alcohol using molecular oxygen over Au-Pd/TiO_2 heterogeneous catalyst. In a flat-membrane microchannel packed-bed reactor, a benzyl alcohol conversion and benzaldehyde selectivity of 70% and 71%, respectively, have been reported under an oxygen pressure of 8.4 bar and a liquid pressure of 10 bar (Wu et al., 2019a). Owing to the unique excellent chemical resistance and thermal stability of Teflon AF-2400 membranes, the aerobic oxidation of benzyl alcohol over a Ru/Al_2O_3 catalyst is efficiently achieved using such a membrane microchannel reactor (Wu et al., 2019b).

Meanwhile, metalloporphyrins have been widely used for the selective aerobic oxidation of organic compounds, such as alkanes, alkenes, and alcohols, etc. in the presence of aldehyde as a co-reductant (Nesterova et al., 2016; Guo et al., 2019; Bugnola et al., 2020; Li et al., 2012; Jiang et al., 2018; Mukherjee and Dey, 2019). Our group has even reported the selective oxidation of alcohols to carbonyl compounds over ruthenium porphyrins with isobutyraldehyde as the oxygen activator in a batch bubble column reactor (Ji et al., 2007; Zhou and Ji, 2012). However, there are still a limited number of studies on the selective aerobic oxidation of alcohols by metalloporphyrins in a continuous microchannel reactor.

Thus, our group decided to investigate the selective aerobic oxidation of benzyl alcohol to benzaldehyde over cobalt porphyrin in a membrane microchannel reactor to examine the feasibility of a continuous flow reactor. In addition, the mechanism for the oxidation of benzyl alcohol was proposed via *in situ* electron paramagnetic resonance (EPR) and *in situ* UV–visible spectroscopy. Notably, a mathematical kinetic model for the membrane microchannel reactor was proposed, which can be beneficial to process optimization and reactor design.

2. Experimental

2.1. Materials

Benzyl alcohol (99.5%), benzaldehyde (99.5%), benzoic acid (99.5%), *N-tert*-butyl-alpha-phenylnitrone (PBN), and isobutyraldehyde (99.9%) were purchased from J&K Scientific (Beijing). Isobutyraldehyde was redistilled before use. Analytical-grade solvent (1,2-dichloroethane, DCE) and other reagents were used without further purification. Cobalt *meso*-tetraphenylporphyrin (CoTPP) was synthesized according to a previously reported procedure (Zhou and Ji, 2010). MALDI-TOF of CoTPP (CH_2Cl_2) [$C_{44}H_{28}CoN_4$]: m/z = 671.5 (exp.), m/z = 671.2 (cal.). UV–vis (CH_2Cl_2) λ_{max} (nm): 465 (Soret band), 590 (Q band). IR: 1638 cm^{-1}, 1001 cm^{-1}, 741 cm^{-1} (Figs. S1–S3).

2.2. Equipment and experimental procedures.

Fig. 1 shows the schematic overview of the experimental setup. The solution containing benzyl alcohol, solvent A (DCE), and the catalyst was delivered by a continuous syringe pump at a flow rate of 2 mL/min (Liquid A). Isobutyraldehyde and solvent B (DCE) were delivered by a continuous syringe pump at a flow rate of 2 mL/min (Liquid B). Liquid A and B were mixed in a T-mixer. Then, the gas and liquid phases were pumped into a membrane microchannel reactor (Vapourtec E, England). Two phases channel were separated using a semipermeable membrane, which permitted the passage of oxygen molecules to the liquid phase. The temperature of the membrane microchannel reactor was monitored by an air heating channel. The oxidation of benzyl alcohol was performed in the membrane microchannel reactor, which was assumed to be a plug-flow reactor. The reaction residence time could be precisely controlled by the solution flow rate.

2.3. Methodology

Operando characterization such as EPR spectroscopy and *in-situ* UV–Vis spectroscopy was conducted under the reaction conditions according to our previous studies (Zhou et al., 2020). The conversion of benzyl alcohol, consumption of isobutyraldehyde, and formation of products were monitored by GC and GC-MS. GC analyses were performed on a Shimadzu GC-2010 Plus chromatography system equipped with anRtx-5 capillary column (30 m × 0.25 mm × 0.25 μm). GC-MS analyses were performed on a Shimadzu GCMS-QP2010 system equipped with a Rxi-5 ms capillary column (30 m × 0.25 mm × 0.25 μm). The CSI-MS spectrometer were obtained on Bruker's timsTOF, and the cold jet is Bruker's CryoSpray. The IR spectra were obtained on a Bruker 550 spectrometer. The UV–vis spectra were recorded on a Shimadzu UV-2450 spectrophotometer.

The rate of reaction was determined by the slope of the curve of the benzyl alcohol residual concentration at different time intervals. The reaction order was obtained by the initial concentration method. All kinetic rate constants were reproducible within an experimental error of ±5%.

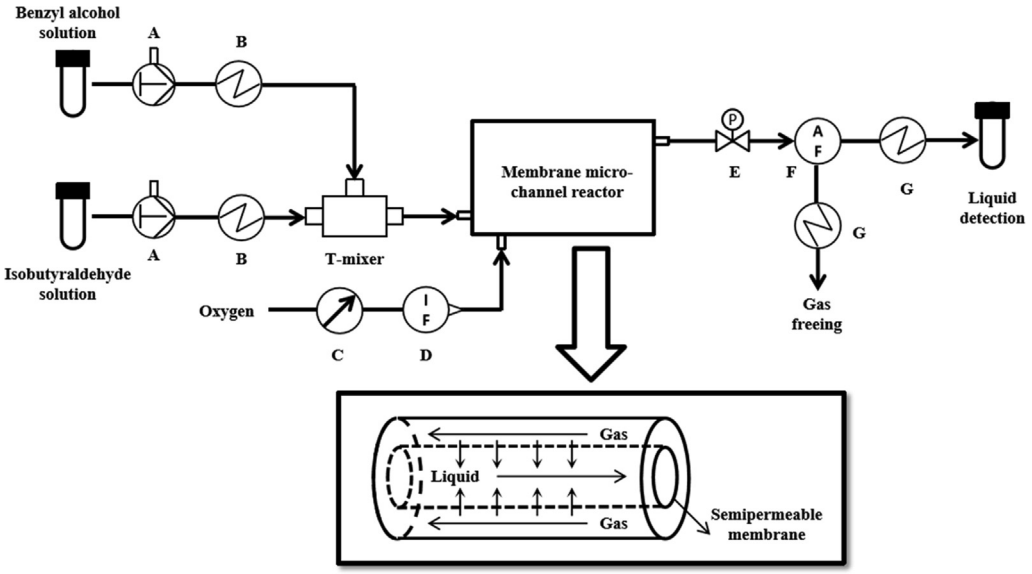

Fig. 1. Schematic overview of the membrane microchannel reactor setup. A:pump, B:preheater, C: gas pressure gage, D: mass-flow controller, E: backpressure valve, F: gas-liquid separator, G:condenser.

3. Results and discussion

3.1. Catalytic oxidation of benzyl alcohol

Fig. 2 shows the reaction profiles for the oxidation of benzyl alcohol catalyzed by CoTPP in the presence of isobutyraldehyde and molecular oxygen. In particular, oxidation was effective in the membrane microchannel reactor. By conducting the reaction in only 6.5 min, the conversion of benzyl alcohol reached 82%. As shown in Fig. 2, during the first 390 s, the conversion of benzyl alcohol was increased continually, meanwhile the selectivity of benzaldehyde and benzoic acid were stable at 94–96% and 4–6% respectively. It was suggested that benzyl alcohol was mostly oxidized to benzaldehyde continually during the period. As the oxidation proceed, the generation of benzoic acid was observed over 480 s. It could be attributed to the deep oxidation of benzaldehyde.

Compared with that observed for the benzyl alcohol oxidation in a bubble column reactor [19], the efficiency was considerably improved, indicating that the membrane microchannel reactor is effective in achieving a rapid gas-liquid mass transfer rate and high mixing performance.

3.2. Effect of temperature on benzyl alcohol oxidation

The effect of the reaction temperature in this membrane microchannel reactor was examined. Fig. 3 showed that the oxidation was greatly influenced by the reaction temperature. With increasing temperature, the conversion of benzyl alcohol was increased. And the selectivity of benzaldehyde was almost at 96%. However, the deep oxidation of benzaldehyde was observed when the reaction temperature was over 65 °C.

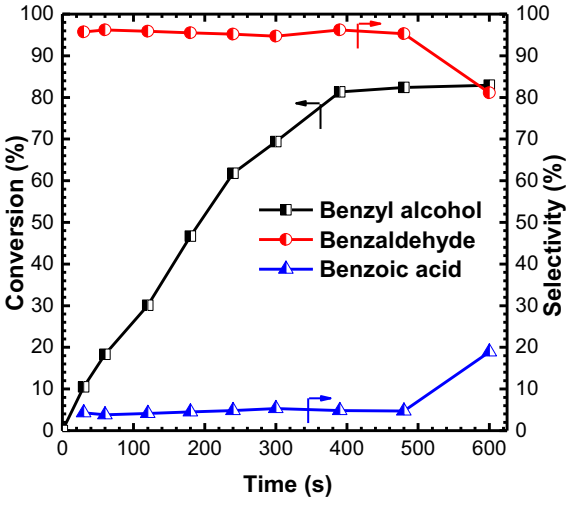

Fig. 2. Reaction profile for the aerobic oxidation of benzyl alcohol catalyzed by CoTPP in the presence of isobutyraldehyde in the membrane microchannel reactor. Benzyl alcohol (0.23 mol/L), isobutyraldehyde (0.92 mol/L), CoTPP (1.80×10^{-4} mol/L), liquid flow (4.0 mL/min), oxygen flow (15 mL/min), 65 °C.

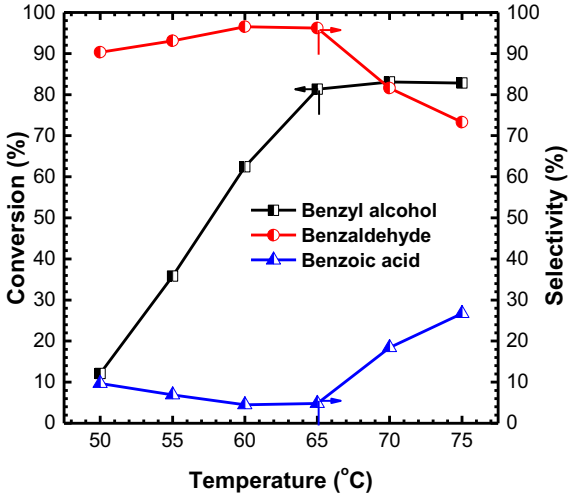

Fig. 3. Effect of the reaction temperature on the oxidation of benzyl alcohol catalyzed by CoTPP in the presence of isobutyraldehyde and molecular oxygen in the membrane microchannel reactor. Benzyl alcohol (0.23 mol/L), isobutyraldehyde (0.92 mol/L), CoTPP (1.80×10^{-4} mol/L), liquid flow (4.0 mL/min), oxygen flow (15 mL/min), 390 s.

When the reaction was conducted at 75 °C, the selectivity for benzoic acid reached up to 27%.

There were the temperature control units in membrane microchannel reactor. Temperature was controlled in set point by air heating and cooling. The temperature profiles of the reactor along reaction time was shown in Fig. 4. It could be observed that the temperature in reactor during the reaction was stable at 65.0 °C. Therefore, reactor system could be considered as isothermal conditions.

3.3. Effect of the amount of catalyst and isobutyraldehyde

Subsequently, the effect of the CoTPP catalyst amount on the selective oxidation of benzyl alcohol was examined in the membrane microchannel reactor. In the control experiment of the catalyst (entry 1 in Table 1), a benzyl alcohol conversion of only 8% was obtained, possibly because a high catalyst concentration led to the improvement in the benzyl alcohol conversion. However, an extremely high catalyst concentrations was conducive to the deep oxidation of benzaldehyde (entries 2–7 in Table 1).

In the catalytic oxidation by metal complexes, isobutyraldehyde was used as a co-substrate to activate dioxygen via the generation of acyl radicals. Therefore, the efficiency of oxidation can be affected by the isobutyraldehyde amount. In the absence of isobutyraldehyde, 10% benzyl alcohol was converted to benzaldehyde with excellent selectivity (entry 8 in Table 1). With the increase in the isobutyraldehyde amount, the conversion increased (entries 9–13 in Table 1). At an isobutyraldehyde concentration of greater than 0.92 mol/L, the conversion did not distinctly improve. Moreover, an excess amount of isobutyraldehyde can result in the decreased selectivity of benzaldehyde.

To examine whether benzaldehyde as the product exhibits the same oxygen activation role as isobutryaldehyde, the oxidation of benzyl alcohol was conducted in the presence of benzaldehyde (entry 14 in Table 1). The same efficiency as that obtained in the control experiment of isobutyraldehyde was observed (entry 8 in Table 1), indicating that benzaldehyde is more inert than isobutyraldehyde for oxygen activation.

3.4. Plausible mechanism for the oxidation of benzyl alcohol

To explore the mechanism for the aerobic oxidation of benzyl alcohol in the presence of CoTPP and isobutyraldehyde in the membrane microchannel reactor, some operando characterization techniques such as *in situ* EPR and UV–vis spectroscopy were performed.

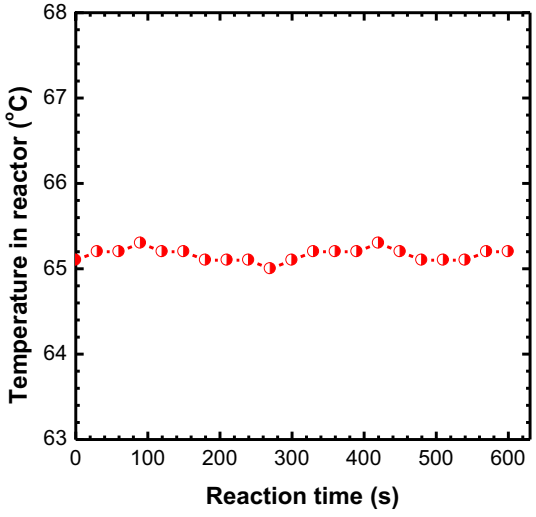

Fig. 4. Temperature profiles in the membrane microchannel reactor over time. Benzyl alcohol (0.23 mol/L), isobutyraldehyde (0.92 mol/L), CoTPP (1.80×10^{-4} mol/L), 65 °C, liquid flow (4.0 mL/min), oxygen flow (15 mL/min), 600 s.

in situ EPR spectra were recorded during the oxidation of benzyl alcohol at a microwave frequency of 9.05 GHz. Benzyl alcohol, catalyst, and DCE were added in a Wilmad WG-810-A quartz-flat cell. First, the mixture in the cell was sealed after filling CO_2 and heated at 65 °C. EPR signals were not observed under CO_2 atmosphere without calefaction (Fig. 5a), indicating that free radicals are absent in the blank of isobutyraldehyde. Then, isobutyraldehyde was added into the reaction system with heating to 65 °C under CO_2 atmosphere, generating a stable DMPO radical adduct (·, a^N = 1.46 mT) (Fig. 5b). Therefore, this free radical is known to be generated from isobutyraldehyde. Previous studies have reported that this free radical is possibly related to the acyl radical, which is generated from the dehydrogenation of isobutyraldehyde by calefaction. Subsequently, the CO_2 atmosphere was replaced by molecular oxygen under the same conditions as described above, and another stable DMPO radical peak adduct was obtained (♣, a^N = 0.80 mT) (Fig. 5c). Acyl radical is a type of active species, which can rapidly react with dioxygen. Hence, this adduct can be assigned tothe peroxyl radical.

Fig. 6 shows the time courses of *in situ* EPR spectra for the oxidation of benzyl alcohol catalyzed by CoTPP in the presence of isobutyraldehyde and molecular oxygen. With the progress of the reaction, the radical transformation from the acyl radical to peroxyl radical was confirmed. By prolonging the reaction even up to 10 min, the acyl radical concentration marginally changed. However, the peroxyl radical concentrationwas significantly high. Hence, the consumption of peroxyl radical can be reasonably concluded to be a limited step for benzyl alcohol oxidation.

Oxidation catalyzed by metalloporphyrins occurred by the oxygen atom-transfer (OAT) mechanism via high-valent species (Sharma et al., 2018; Cho et al., 2016; Liu et al., 2020). The intermediate formed during oxidation can be characterized by UV–vis absorption spectroscopy. Fig. 7 shows the time courses of the *in situ* UV–vis spectrum for the oxidation of benzyl alcohol under the given reaction conditions. In the initial reaction period, a clear absorption peak at 465 nm (Soret band) was observed, corresponding to Co^{II}TPP. With the progress of oxidation, the absorption peak gradually decreased, accompanied with the gradual increase in a new absorption peak at 486 nm. This peak corresponded to cobalt high-valent species (Co^{III} = OTPP), indicative of the combination between peroxyl radical and Co^{II}TPP.

Based on the above discussion, the mechanism for the aerobic oxidation of benzyl alcohol by Co^{II}TPP and isobutyraldehyde in a membrane microchannel reactor was proposed (Fig. 8). The dehydrogenation of isobutyraldehyde to the acyl radical primarily occurred under reaction conditions (a). Then, one oxygen molecule combined with the acyl radical to generate a peroxyl radical (b). Subsequently, Co^{III} = OTPP (d) was generated by the combination of peroxyl acid(c) and Co^{II}TPP. The formation of benzaldehyde corresponded to the reaction between benzyl alcohol and Co^{III} = OTPP, followed by β-hydride elimination(pathway A). The catalyst blank exhibited a conversion of 8% (entry 1 in Table 1), corresponding to the reaction between peroxyl acid and benzyl alcohol (pathway B).

3.5. Kinetic studies

To eliminate the influence of mass transfer in the membrane microchannel reactor, oxidation was conducted under various oxygen flows from 0.5 to 3.8 mL/min. The oxygen flow exerted a slight effect on the reaction (Fig. S4). Because the membrane microchannel is a type of reactor that can considerably improve the gas-liquid mass-transfer efficiency, the gas-liquid mass transfer in the reactor can be eliminated. Fig. 9 plots a typical concentration profile for the

Table 1
Effect of the amount of catalyst and isobutyraldehyde on the oxidation of benzyl alcohol.[a]

Entry	Catalyst ($\times 10^{-4}$ mol/L)	Isobutyraldehyde(mol/L)	Conversion/%	Selectivity/%	
				Benzaldehyde	Benzoic acid
1	0	0.92	8	31	69
2	0.45	0.92	32	96	4
3	0.90	0.92	60	97	3
4	1.35	0.92	80	96	4
5	1.80	0.92	82	98	2
6	2.25	0.92	86	94	6
7	2.70	0.92	88	91	9
8	1.80	0	10	99	1
9	1.80	0.23	60	97	3
10	1.80	0.46	71	97	3
11	1.80	0.69	80	96	4
12	1.80	1.15	81	92	8
13	1.80	1.38	82	88	12
14[b]	1.80	0	10	>99	–

[a] Benzyl alcohol (0.23 mol/L), 65 °C, liquid flow (4.0 mL/min), oxygen flow (15 mL/min), 390 s.
[b] In the presence of benzaldehyde (0.92 mol/L).

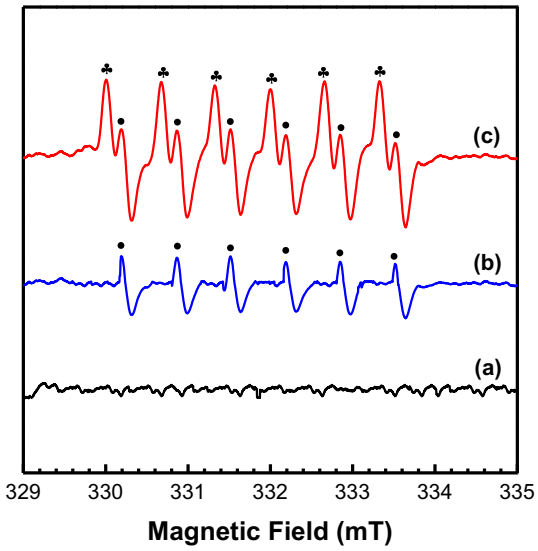

Fig. 5. *in situ* EPR spectra for the oxidation of benzyl alcohol catalyzed by CoTPP at 65 °C. (a) In the absence of isobutyraldehyde under CO_2 atmosphere; (b) in the presence of isobutyraldehyde under CO_2 atmosphere; (c) in the presence of isobutyraldehyde under O_2 atmosphere.

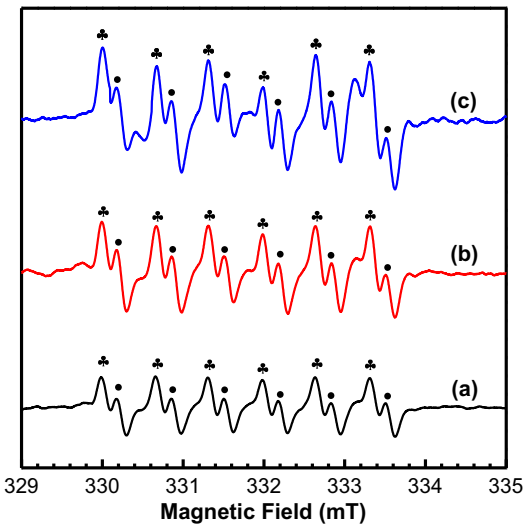

Fig. 6. Time courses of *in situ* EPR spectra for the aerobic oxidation of benzyl alcohol catalyzed by CoTPP in the presence of isobutyraldehyde at 65 °C. (a) 1.0 min; (b) 5.0 min; and (c) 10 min.

oxidation of benzyl alcohol catalyzed by CoTPP in the membrane microchannel reactor. Almost 4 equivalents of isobutyraldehyde was consumed to obtain 1 equivalent of benzaldehyde. Therefore, the autooxidation of isobutyraldehyde under the reaction conditions cannot be excluded.

In the presence of isobutyraldehyde and molecular oxygen in the membrane microchannel reactor, the oxidation of two substrates, i.e., benzyl alcohol and isobutyraldehyde, respectively, was catalyzed by cobalt porphyrin. Following the reaction mechanism shown in Fig. 8, the reaction equations were listed as below:

Radical-chain initiation:

$$\mathrm{iPrCHO} \xrightarrow{k_1} + \mathrm{iPrCO}\cdot + \mathrm{H}\cdot \quad (1)$$

Radical-chain propagation:

$$\mathrm{iPrCO}\cdot + \mathrm{O_2} \xrightarrow{k_2} \mathrm{iPrCO_3} \quad (2)$$

$$\mathrm{iPrCO_3}\cdot + \mathrm{iPrCHO} \xrightarrow{k_3} \mathrm{iPrCO_3H} + \mathrm{iPrCO}\cdot \quad (3)$$

$$\mathrm{PorCo^{II}} + \mathrm{iPrCO_3H} \xrightarrow{k_4} \mathrm{PorCo^{III}} = \mathrm{O} + \mathrm{iPrCOOH} \quad (4)$$

$$\mathrm{iPrCO_3H} + \mathrm{PhCH_2OH} \xrightarrow{k_5} \mathrm{iPrCOOH} + \mathrm{PhCHO} \quad (5)$$

$$\mathrm{PorCo^{III}} = \mathrm{O} + \mathrm{PhCH_2OH} \xrightarrow{k_6} \mathrm{PorCo^{II}} + \mathrm{PhCHO} \quad (6)$$

$$\mathrm{iPrCO_3H} + \mathrm{iPrCHO} \xrightarrow{k_7} 2\mathrm{iPrCOOH} \quad (7)$$

$$\mathrm{PorCo^{III}} = \mathrm{O} + \mathrm{iPrCHO} \xrightarrow{k_8} \mathrm{PorCo^{II}} + \mathrm{iPrCOOH} \quad (8)$$

Radical-chain termination:

$$\mathrm{H}\cdot + \mathrm{iPrCO}\cdot \xrightarrow{k_9} \mathrm{inactive} \quad (9)$$

$$2\mathrm{iPrCO}\cdot \xrightarrow{k_{11}} \mathrm{inactive} \quad (10)$$

According to the reaction equations Eqs. (1)–(10), the molar balance equations for the free-radical component can be expressed as shown in Eqs. (11)–(14). The system was assumed to be in the

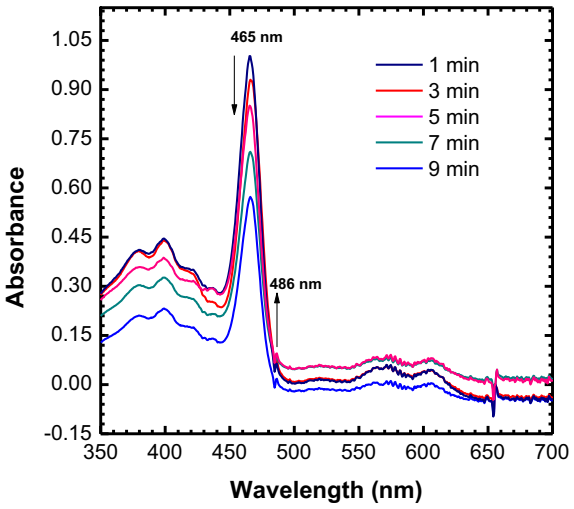

Fig. 7. *in situ* UV–vis spectra for the oxidation of benzyl alcohol by CoTPP in the presence of isobutyraldehyde and molecular oxygen. Benzyl alcohol (0.23 mol/L), isobutyraldehyde (0.92 mol/L), CoTPP (1.8×10^{-4} mol/L), liquid flow (4.0 mL/min), oxygen flow (15 mL/min).

pseudo-steady-state, and the production of the free-radical component was balanced by its consumption. Therefore, the reaction rate for the free-radical component is zero.

$$\frac{d[iPrCO\cdot]}{dt} = k_1[iPrCHO] - k_2[iPrCO\cdot][O_2] + k_3[iPrCO_3\cdot][iPrCHO] - k_{11}[iPrCO\cdot]^2 = 0 \quad (11)$$

$$\frac{d[iPrCO_3\cdot]}{dt} = k_2[iPrCO\cdot][O_2] - k_3[iPrCO_3\cdot][iPrCHO] = 0 \quad (12)$$

$$\frac{d[iPrCO_3H]}{dt} = k_3[iPrCO_3\cdot][iPrCHO] - k_4[PorCo^{II}][iPrCO_3H] - k_5[iPrCO_3H][PhCH_2OH] - k_7[iPrCO_3H][iPrCHO] = 0 \quad (13)$$

$$\frac{d[PorCo^{III}=O]}{dt} = k_4[PorCo^{II}][iPrCO_3H] - k_6[PorCo^{III}=O][PhCH_2OH] - k_8[PorCo^{III}=O][iPrCHO] = 0 \quad (14)$$

According to the dynamitic model of deriving, the generation rate of benzaldehyde could be derived as shown in Eq. (15).

$$\frac{d[PhCHO]}{dt} = \left\{k_5 + \frac{k_4k_6[PorCo^{II}]}{k_6[PhCH_2OH] + k_8[iPrCHO]}\right\} \times \frac{k_2\left(\frac{k_1}{k_{11}}\right)^{\frac{1}{2}}[O_2][iPrCHO]^{\frac{1}{2}}[PhCH_2OH]}{k_4[PorCo^{II}] + k_5[PhCH_2OH] + k_7[iPrCHO]} \quad (15)$$

In the catalytic reaction system, the amount of catalyst ($ProCo^{II}$) was about one-thousandth that of the other reagents. Hence, the concentrations of the catalyst ($ProCo^{II}$) and high-valent species ($ProCo^{III}$ = O) can be negligible. Then, the generation rate of benzaldehyde can be simplified as shown in Eq. (16).

$$\frac{d[PhCHO]}{dt} = -\frac{k_2k_5\left(\frac{k_1}{k_{11}}\right)^{\frac{1}{2}}[O_2][iPrCHO]^{\frac{1}{2}}[PhCH_2OH]}{[PhCH_2OH] + \frac{k_7}{k_5}[iPrCHO]} \quad (16)$$

Under the reaction conditions, oxygen was continuously fed, indicating that the O_2 concentration remains constant during the reaction. Then, K_1 is defined as follows:

$$K_1 = -k_2k_5\left(\frac{k_1}{k_{11}}\right)^{\frac{1}{2}}[O_2] \quad (17)$$

$$K_2 = \frac{k_7}{k_5} \quad (18)$$

Therefore, the generation rate of benzaldehyde can be derived as shown in Eq. (19).

$$\frac{d[PhCHO]}{dt} = \frac{K_1[iPrCHO]^{\frac{1}{2}}[PhCH_2OH]}{[PhCH_2OH] + K_2[iPrCHO]} \quad (19)$$

From Eq. (19), the generation rate of benzaldehyde was related to the concentrations of benzyl alcohol and isobutyraldehyde. From the above discussion, the amount of isobutyraldehyde was

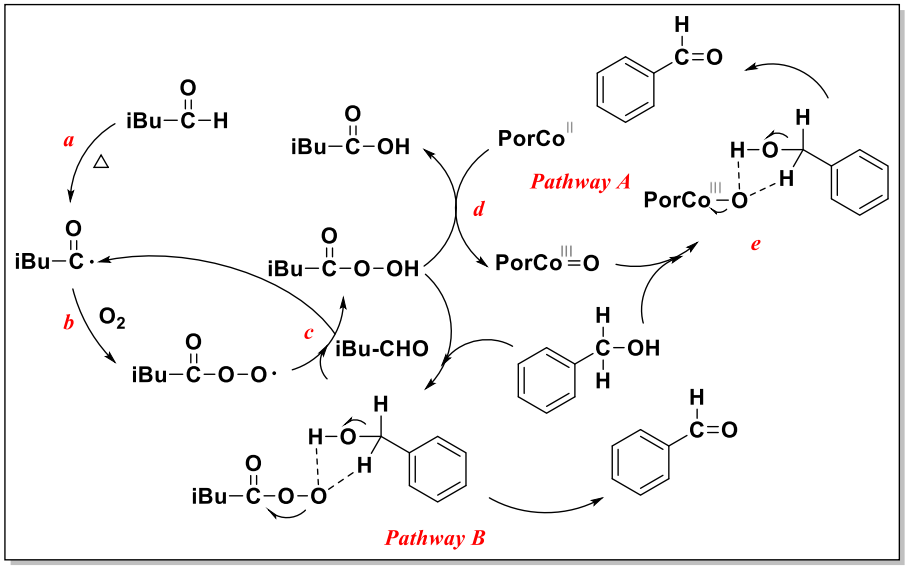

Fig. 8. Plausible mechanism for the oxidation of benzyl alcohol catalyzed by CoTPP with dioxygen and isobutyraldehyde in a membrane microchannel reactor.

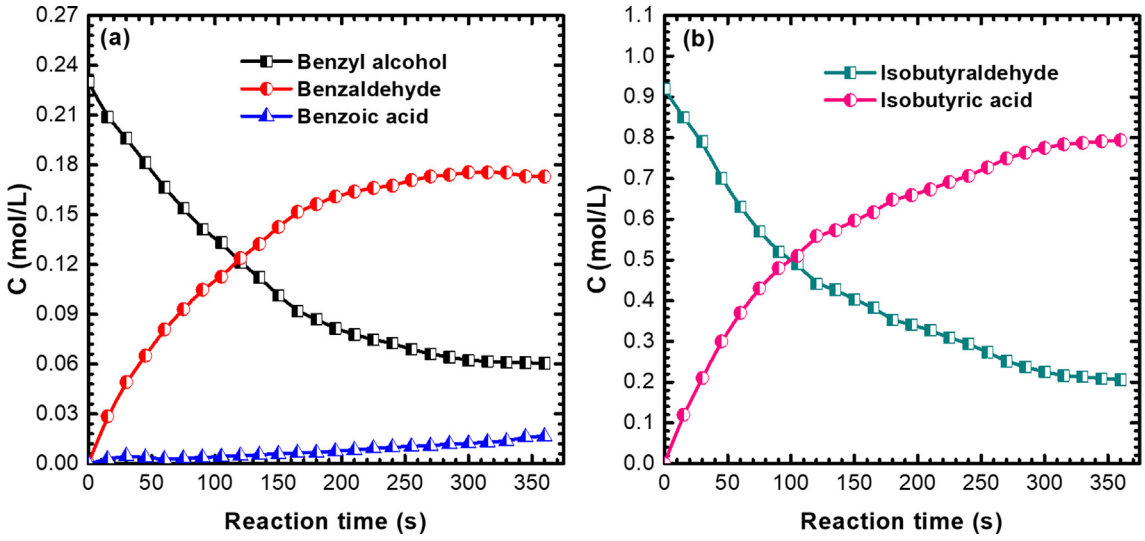

Fig. 9. Concentration profiles for the oxidation of benzyl alcohol catalyzed by CoTPP in the membrane microchannel reactor in the presence of isobutyraldeyde and molecular oxygen (a: consumption of benzyl alcohol; b: consumption of isobutyraldehyde). Benzyl alcohol (0.23 mol/L), isobutyraldehyde (0.92 mol/L), CoTPP (1.8×10^{-4} mol/L), 65 °C, liquid flow (4.0 mL/min), oxygen flow (15 mL/min).

considerably greater than that of benzyl alcohol, and a marginal amount of isobutyraldehyde is consumed for participation in oxidation, indicating that the isobutyraldehyde concentration remains constant during the reaction.

Consequently, the reaction rate for different reactant concentrations was examined (Fig. 10a). The reaction rate constants were obtained by the initial concentration method (Figs. S5–S10, Table S1). The activation energy (E_a) was calculated by Arrhenius equation fitting, and its value was 70.3 kJ/mol (Fig. S11–12).

The oxidation of benzyl alcohol was found to be a first-order reaction at a low substrate concentration. However, with the increase in the concentrations of benzyl alcohol in the range of 0.6–1.0 mol/L, the benzyl alcohol concentration exhibited a negative linear relationship with reaction time (Fig. S13), indicating that the reaction rate does not change with the reactant concentrations. Moreover, at high substrate concentrations, the reaction rate was almost zero order.

Therefore, the obtained kinetic equation (Eq. (19)) is comparable to the Michaelis–Menten-type kinetics from expression Eq. (20),

$$\frac{1}{v} = \frac{K_m}{v_{max}} \frac{1}{[S]} + \frac{1}{v_{max}} \tag{20}$$

where v and $[S]$ represent the reaction rate and benzyl alcohol concentration of catalytic oxidation, respectively. v_{max} represents the maximum reaction rate with a specific catalyst concentration. In enzyme-catalyzed reactions, K_m represents the magnitude of the affinity between the enzyme and reactant. With the decrease in K_m, the affinity increases.

Next, the steady-state kinetic model of the catalytic system was evaluated by the Lineweaver–Burk plot. The reaction rate (v) was determined via the reducing concentration of benzyl alcohol ($[S]$). A good linear relationship was obtained for $1/v$ versus $1/[S]$ (Fig. 10b). The slope and intercept of the plot revealed a v_{max} of 0.00272 mol·L^{-1}·min^{-1} and a K_m of 0.133 mol·L^{-1}. The K_m value is far less than that for H_2O_2 catalase (K_m = 1.1 mol·L^{-1}) in living organisms, indicating that there is a strong affinity between the cobalt porphyrin catalyst and benzyl alcohol in this catalytic oxidation.

Hence, the kinetic behavior for the oxidation of benzyl alcohol follows the Michaelis–Menten kinetics. The kinetic model for the oxidation of benzyl alcohol catalyzed by cobalt porphyrin in the presence of isobutyraldehyde in the membrane microchannel reactor is expressed as shown in Eq. (21).

$$v = \frac{0.00272[S]}{0.133 + [S]} \tag{21}$$

The obtained kinetic model for biomimetic catalytic oxidation was verified with different initial concentrations of benzyl alcohol. The lines fitted the experimental data extremely well for a low initial concentration of benzyl alcohol (Fig. 11). However, at a higher initial concentration of benzyl alcohol, the experimental data were not in good agreement with the calculated data. When the initial concentration of benzyl alcohol was greater than 0.80 mol/L, a substantial deviation was observed between the experimental data and predicted data using the existing Michaelis–Menten kinetics, possibly related to the negligible effect of isobutyraldehyde on the reaction rate. As discussed above, the isobutyraldehyde concentration significantly affected the generation rate of benzaldehyde. Hence, the isobutyraldehyde concentration could not be regarded as a constant in the kinetic model.

The model derived from the mechanism includes the variable of the isobutyraldehyde concentration (Eq. (19)). By the comparison of Eq. (19) and Eq. (21),

$$\mathrm{v_{max}} = 0.00272 = K_1[\mathrm{iPrCHO}]^{\frac{1}{2}}, K_m = 0.133 = \mathrm{K_2[iPrCHO]} \tag{22}$$

Therefore, K_1 and $K_m$can be determined on the basis of the benzyl alcohol and isobutyraldehyde concentrations during the reaction. For example, the measured benzyl alcohol concentration was 0.25 mol/L, and the isobutyraldehyde concentration was 1.21 mol/L. Accordingly, K_1 = 0.0025, K_2 = 0.1099 mol/L.

Hence, Eq. (23) is rewritten as follows:

$$\mathrm{v} = \frac{0.0025[\mathrm{iPrCHO}]^{\frac{1}{2}}[\mathrm{PhCH_2OH}]}{[\mathrm{PhCH_2OH}] + 0.1099[\mathrm{iPrCHO}]} \tag{23}$$

Then, the modified kinetic model for biomimetic catalytic oxidation was verified with different initial concentrations of benzyl alcohol. The lines fitted the experimental data very well irrespective of the low and high benzyl alcohol concentrations (Fig. 12). Therefore, this mathematical model can predict the reaction pro-

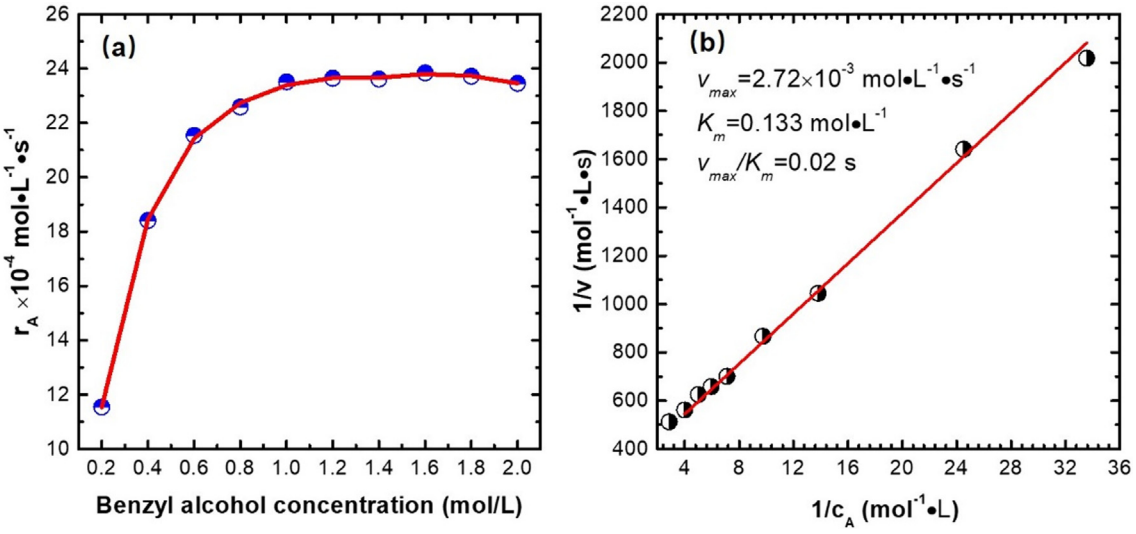

Fig.10. (a) Curve for the reaction rate vs benzyl alcohol concentration, and (b) Lineweaver–Burk plots for the oxidation of benzyl alcohol catalyzed by CoTPP.

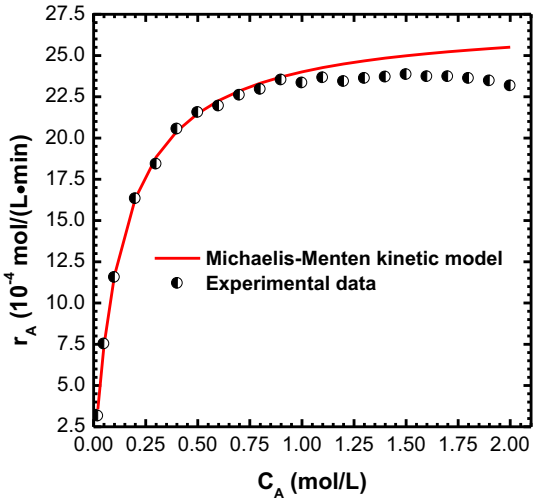

Fig. 11. Comparison of the Michaelis–Menten kinetic model and experimental data at different initial concentrations of benzyl alcohol.

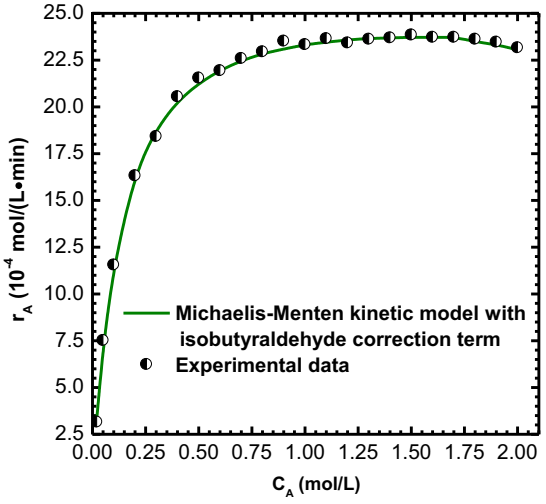

Fig. 12. Comparison of the calculated model (Eq. (25)) and experimental data on the relationship between the oxidation rate and benzyl alcohol concentration.

cess in a wide range of benzyl alcohol concentrations, which can serve as a reference to design a pilot reactor and for the optimization of a process.

3.6. Mass transfer

To definite the gas-liquid mass transfer effect in the membrane micro-channel reactor, liquid-film mass transfer coefficients (k_La)

Table 2
Continuous reaction liquid film mass transfer coefficient.[a]

Air flow (mL/min)	v_1-v_2 (mL/min)	V_A (mL)	C_O^*-C_O (mg/L)	k_La (min^{-1})
10	5.8	0.64	14.9	318.7
15	6.7	0.64	18.7	358.3
20	3.6	0.64	14.1	428.3
25	3.9	0.64	13.8	554.5
30	3.7	0.64	10.7	665.8

[a] Benzyl alcohol (0.23 mol/L), 65 °C, liquid flow (4.0 mL/min), oxygen flow (15 mL/min), 390 s.

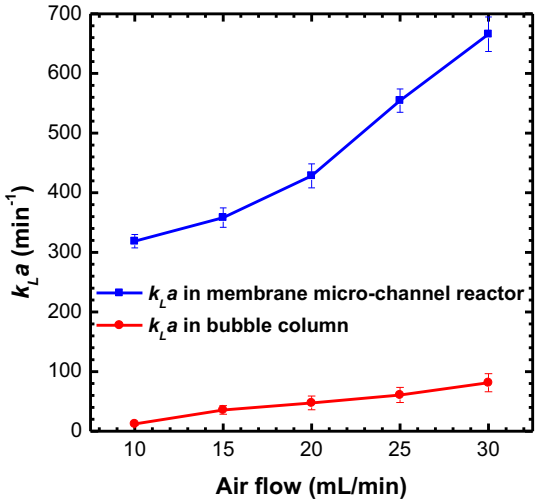

Fig. 13. Comparison of liquid-film mass transfer coefficients between membrane micro-channel reactor and bubble column. Benzyl alcohol (0.23 mol/L), isobutyraldehyde (0.92 mol/L), CoTPP (1.8 × 10–4 mol/L), 65 °C, liquid flow (4.0 mL/min), 390 s.

was calculated by Eq. (24) and its parameter calculation was shown in Table 2.

$$N_{O_2} = k_L a \cdot (C^* - C_0) = \frac{v_1 - v_2}{V} \quad (24)$$

The $k_L a$ value changed with air flow was shown in Fig. 13. It was found that the liquid-film mass transfer coefficients in the membrane micro-channel reactor were in the range of 318–666 min^{-1}. Instead it was just in the range of 12–81 min^{-1} in bubble column. The enormous difference between the two reactors showed the advantages in gas-liquid mass transfer of membrane micro-channel reactor. Membrane micro-channel reactor could provide more gas-liquid contact area, which was conducive to the diffusion of oxygen in liquid film.

4. Conclusion

In conclusion, the selective aerobic oxidation of benzyl alcohol catalyzed by cobalt porphyrin was performed in a membrane microchannel reactor. The efficiency for the oxidation of benzyl alcohol performed in a microstructured chemical system improved the efficiency in a short reaction time. Based on the results obtained from experiments as well as *in situ* EPR and UV–vis spectra, a plausible mechanism for the oxidation of benzyl alcohol catalyzed by cobalt porphyrin in presence of isobutyraldehyde was proposed. Furthermore, kinetic studies revealed that the oxidation of benzyl alcohol follows the Michaelis–Menten kinetics, with K_m = 0.133 mol/L. The low K_m value represented the strong affinity between the catalyst and benzyl alcohol. A mathematic kinetic model was proposed, and the kinetic model fitted the experimental data well. The mathematical model can predict the reaction process in a wide range of benzyl alcohol concentrations, which is beneficial for the process optimization and reactor design.

CRediT authorship contribution statement

Qi Han: Conceptualization, Investigation, Writing - original draft. **Xian-Tai Zhou:** Supervision, Writing - review & editing, Funding acquisition. **Xiao-Qi He:** Conceptualization, Methodology. **Hong-Bing Ji:** Project administration, Funding acquisition.

Declaration of Competing Interest

The authors declare that they have no known competing financial interests or personal relationships that could have appeared to influence the work reported in this paper.

Acknowledgements

This work was financially supported by the National Key Research and Development Program of China (2020YFA0210900), the National Natural Science Foundation of China (No. 21938001, 21878344 and 21961160741), the National Natural Science Foundation of China-SINOPEC Joint Fund (No. U1663220), Guangdong Provincial Key R&D Programme (2019B110206002), the Local Innovative and Research Teams Project of Guangdong Pearl River Talents Program (2017BT01C102), Research and Innovation Team Construction Project of Guangdong University of Petrochemical Technology (2019rc049), Science and Technology Project of Huizhou (2017X0103003 and 2017G0516063).

Appendix A. Supplementary material

Supplementary data to this article can be found online at https://doi.org/10.1016/j.ces.2021.116847.

References

Al-Rifai, N., Galvanin, F., Morad, M., Cao, E.H., Cattaneo, S., Sankar, M., Dua, V., Hutchings, G., Gavriilidis, A., 2016. Hydrodynamic effects on three phase micro-packed bed reactor performance -gold-palladium catalysed benzyl alcohol oxidation. Chem. Eng. Sci. 149, 129–142.

Bawornruttanaboonya, K., Devahastin, S., Mujumdar, A.S., Laosiripojana, N., 2017. A computational fluid dynamic evaluation of a new microreactor design for catalytic partial oxidation of methane. Int. J. Heat Mass Transf. 115, 174–185.

Bugnola, M., Shen, K.J., Haviv, E., Neumann, R., 2020. Reductive electrochemical activation of molecular oxygen catalyzed by an iron-tungstate oxide capsule: reactivity studies consistent with compound I type oxidants. ACS Catal. 10, 4227–4237.

Cang, R.B., Lu, B., Li, X.P., Niu, R., Zhao, J.X., Cai, Q.H., 2015. Iron-chloride ionic liquid immobilized on SBA-15 for solvent-free oxidation of benzyl alcohol to benzaldehyde with H_2O_2. Chem. Eng. Sci. 137, 268–275.

Cerdan, K., Ouyang, W.Y., Colmenares, J.C., Munoz-Batista, M.J., Luque, R., Balu, A.M., 2019. Facile mechanochemical modification of g-C_3N_4 for selective photo-oxidation of benzyl alcohol. Chem. Eng. Sci. 194, 78–84.

Cho, K.B., Hirao, H., Shaik, S., Nam, W., 2016. To rebound or dissociate? This is the mechanistic question in C-H hydroxylation by heme and nonheme metal-oxo complexes. Chem. Soc. Rev. 45, 1197–1210.

Dai, X., Zhou, W.Y., Yang, S., Sun, F.A., Qian, J.F., He, M.Y., Chen, Q., 2019. Microchannel process for phenol production via the cleavage of cumene hydroperoxide. Chem. Eng. Sci. 199, 398–404.

Denekamp, I.M., Antens, M., Slot, T.K., Rothenberg, G., 2018. Selective catalytic oxidation of cyclohexene with molecular oxygen: radical versus nonradical pathways. ChemCatChem 10, 1035–1041.

Di Somma, I., Russo, D., Andreozzi, R., Marotta, R., Guido, S., 2017. Kinetic modelling of benzyl alcohol selective oxidation in aqueous mixtures of nitric and sulfuric acids. Chem. Eng. J. 308, 738–744.

Eisenberg, D., Slot, T.K., Rothenberg, G., 2018. Understanding oxygen activation on metal-and nitrogen-codoped carbon catalysts. ACS Catal. 8, 8618–8629.

Frija, L.M.T., Kuznetsov, M.L., Rocha, B.G.M., Cabral, L., Cristiano, M.L.S., Kopylovich, M.N., Pombeiro, A.J.L., 2017. Organocatalyzed oxidation of benzyl alcohols by a tetrazole-amino- saccharin: a combined experimental and theoretical (DFT) study. Mol. Catal. 442, 57–65.

Fu, Y., Guo, Y.L., Guo, Y., Wang, Y.S., Wang, L., Zhan, W.C., Lu, G.Z., 2017. In situ assembly of ultrafine Mn_3O_4 nanoparticles into MIL-101 for selective aerobic oxidation. Catal. Sci. Technol. 7, 4136–4144.

Groppo, E., Lazzarini, A., Carosso, M., Bugaev, A., Manzoli, M., Pellegrini, R., Lamberti, C., Banerjee, D., Longo, A., 2018. Dynamic behavior of Pd/P4VP catalyst during the aerobic oxidation of 2-propanol: asimultaneous SAXS/XAS/MS operand study. ACS Catal. 8, 6870–6881.

Guo, M.L., Li, H.Z., 2007. Selective oxidation of benzyl alcohol to benzaldehyde with hydrogen peroxide over tetra-alkylpyridinium octamolybdate catalysts. Green Chem. 9, 421–423.

Guo, M., Seo, M.S., Lee, Y.M., Fukuzumi, S., Nam, W., 2019. Highly reactive manganese(IV)-oxo porphyrins showing temperature-dependent reversed electronic effect in C-H bond activation reactions. J. Am. Chem. Soc. 141, 12187–12191.

Han, Q., Guo, X.X., Zhou, X.T., Ji, H.B., 2020. Efficient selective oxidation of alcohols to carbonyl compounds catalyzed by Ru-terpyridine complexes with molecular oxygen. Inorg. Chem.Commun. 112.

Hu, Y.P., Dong, C., Wang, T., Luo, G.S., 2018. Cyclohexanone ammoximation over TS-1 catalyst without organic solvent in a microreaction system. Chem. Eng. Sci. 187, 60–66.

Ide, Y., Tominaka, S., Kono, H., Ram, R., Machida, A., Tsunoji, N., 2018. Zeolitic intralayer microchannels of magadiite, a natural layered silicate, to boost green organic synthesis. Chem. Sci. 9, 8637–8643.

Ji, H.B., Ebitani, K., Mizugaki, T., Kaneda, K., 2003. Oxidation of benzyl alcohol aiming at a greener reaction. React. Kinet. Catal. Lett. 78, 73–80.

Ji, H.B., Yuan, Q.L., Zhou, X.T., Pei, L.X., Wang, L.F., 2007. Highly efficient selective oxidation of alcohols to carbonyl compounds catalyzed by ruthenium(III) meso-tetraphenylporphyrin chloride in the presence of molecular oxygen. Bioorg. Med. Chem. Lett. 17, 6364–6368.

Jiang, J., Wang, J.X., Zhou, X.T., Chen, H.Y., Ji, H.B., 2018. Mechanistic understanding towards the role of cyclohexene in enhancing the efficiency of manganese porphyrin-catalyzed aerobic oxidation of diphenylmethane. Eur. J. Inorg. Chem. 23, 2666–2674.

Jing, L., Shi, J., Zhang, F.M., Zhong, Y.J., Zhu, W.D., 2013. Polyoxometalate-based amphiphilic catalysts for selective oxidation of benzyl alcohol with hydrogen peroxide under organic solvent-free conditions. Ind. Eng. Chem. Res. 52, 10095–10104.

Kobayashi, J., Mori, Y., Kobayashi, S., 2006. Multiphase organic synthesis in microchannel reactors. Chem. Asian J. 1, 22–35.

Li, H., Qin, F., Yang, Z.P., Cui, X.M., Wang, J.F., Zhang, L.Z., 2017. New reaction pathway induced by plasmon for selective benzyl alcohol oxidation on BiOCl possessing oxygen vacancies. J. Am. Chem. Soc. 139, 3513–3521.

Li, Y., Zhou, X.T., Ji, H.B., 2012. Cocatalytic effect of cobalt acetate on aerobic cyclohexene oxidation catalyzed by manganese porphyrin. Catal. Commun. 27, 169–173.

Liu, C.-H., Lin, C.-Y., Chen, J.-L., Lu, K.-T., Lee, J.-F., Chen, J.-M., 2017. SBA-15-supported Pd catalysts: The effect of pretreatment conditions on particle size and its application to benzyl alcohol oxidation. J. Catal. 350, 21–29.

Liu, Q., Qiu, W., Wu, P., Yue, H., Liu, C., Jiang, W., 2019. Low-temperature ammonia oxidation in a microchannel reactor with wall-loaded X(X = Pt, Pd, Rh, PtPdRh)/TiO_2nanotube catalysts. Ind. Eng. Chem. Res. 58, 9819–9828.
Liu, X.H., Yu, H.Y., Xue, C., Zhou, X.T., Ji, H.B., 2020. Cyclohexene promoted efficient biomimetic oxidation of alcohols to carbonyl compounds catalyzed by manganese porphyrin under mild conditions. Chin. J. Chem. 38, 458–464.
Liu, G.Q., Zhao, C.J., Wang, G.Z., Zhang, Y.X., Zhang, H.M., 2018. Efficiently electrocatalytic oxidation of benzyl alcohol for energy-saved zinc-air battery using a multifunctional nickel-cobalt alloy electrocatalyst. J. Colloid Interface Sci. 532, 37–46.
Ma, Y.Y., Gan, J., Pan, M.J., Zhang, Y.F., Fu, W.Z., Duan, X.Z., Chen, W.Y., Chen, D., Qian, G., Zhou, X.G., 2019. Reaction mechanism and kinetics for Pt/CNTs catalyzed base-free oxidation of glycerol. Chem. Eng. Sci. 203, 228–236.
Mallat, T., Baiker, A., 2004. Oxidation of alcohols with molecular oxygen on solid catalysts. Chem. Rev. 104, 3037–3058.
Meng, Y.T., Genuino, H.C., Kuo, C.H., Huang, H., Chen, S.Y., Zhang, L.C., Rossi, A., Suib, S.L., 2013. One-step hydrothermal synthesis of manganese-containing MFI-type zeolite, Mn-ZSM-5, characterization, and catalytic oxidation of hydrocarbons. J. Am. Chem. Soc. 135, 8594–8605.
Mukherjee, M., Dey, A., 2019. Electron transfer control of reductase versus monooxygenase: catalytic C-H bond hydroxylation and alkene epoxidation by molecular oxygen. ACS Central Sci. 5, 671–682.
Nesterova, O.V., Kopylovich, M.N., Nesterov, D.S., 2016. Stereoselective oxidation of alkanes with m-CPBA as an oxidant and cobalt complex with isoindole-based ligands as catalysts. RSC Adv. 6, 93756–93767.
Olenin, A.Y., Mingalev, P.G., Lisichkin, G.V., 2018. Partial catalytic oxidation of alcohols: catalysts based on metals and metal coordination compounds (a review). Petrol. Chem. 58, 577–592.
Othman, N.H., Wu, Z.T., Li, K., 2015. Micro-structured $Bi_{1.5}Y_{0.3}Sm_{0.2}O_3$- catalysts for oxidative coupling of methane. AIChE J. 61, 3451–3458.
Rebrov, E.V., Duisters, T., Lob, P., Meuldijk, J., Hessel, V., 2012. Enhancement of the liquid-side mass transfer in a falling film catalytic microreactor by in-channel mixing structures. Ind. Eng. Chem. Res. 51, 8719–8725.
Sankar, M., He, Q., Engel, R.V., Sainna, M.A., Logsdail, A.J., Roldan, A., Willock, D.J., Agarwal, N., Kiely, C.J., Hutchings, G.J., 2020. Role of the support in gold-containing nanoparticles as heterogeneous catalysts. Chem. Rev. 120, 3890–3938.
Sarmah, P., Das, B.K., Phukan, P., 2010. Novel dicopper(II)-tetracarboxylates as catalysts for selective oxidation of benzyl alcohols with aqueous TBHP. Catal. Commun. 11, 932–935.
Satrio, J.A.B., Doraiswamy, L.K., 2002. Phase-transfcr catalysis: a new rigorous mechanistic model for liquid-liquid systems. Chem. Eng. Sci. 57, 1355–1377.
Schonfeld, H., Hunger, K., Cecilia, R., Kunz, U., 2004. Enhanced mass transfer using a novel polymer/carrier microreactor. Chem. Eng. J. 101, 455–463.
Sharaf, O.Z., Al-Khateeb, A.N., Kyritsis, D.C., Abu-Nada, E., 2019. Numerical investigation of nanofluid particle migration and convective heat transfer in microchannels using an Eulerian-Lagrangian approach. J. Fluid Mech. 878, 62–97.
Sharma, N., Jung, J., Ohkubo, K., Lee, Y.M., El-Khouly, M.E., Nam, W., Fukuzumi, S., 2018. Long-lived photoexcited state of a Mn(IV)-oxo complex binding scandium ions that is capable of hydroxylating benzene. J. Am. Chem. Soc. 140, 8405–8409.
Shen, C., Wang, Y.J., Xu, J.H., Luo, G.S., 2015. Glass capillaries with TiO_2 supported on inner wall as microchannel reactors. Chem. Eng. J. 277, 48–55.
Snytnikov, P.V., Potemkin, D.I., Rebrov, E.V., Sobyanin, V.A., Hessel, V., Schouten, J.C., 2010. Design, scale-out, and operation of a microchannel reactor with a Cu/CeO_{2-x} catalytic coating for preferential CO oxidation. Chem. Eng. J. 160, 923–929.
Tabakova, T., 2019. Recent advances in design of gold-based catalysts for H_2clean-up reactions. Front. Chem. 7, 1–24.
Torbina, V.V., Vodyankin, A.A., Ten, S., Mamontov, G.V., Salaev, M.A., Sobolev, V.I., Vodyankina, O.V., 2018. Ag-Based Catalysts in heterogeneous selective oxidation of alcohols: areview. Catalysts 8, 449–603.
Venkateswaran, S., Wilhite, B., Kravaris, C., 2019. Optimal heating profiles in tubular reactors with solid-phase axial wall conduction for isothermal operation. AIChE J. 65, 2–14.
Vina-Gonzalez, J., Jimenez-Lalana, D., Sancho, F., Serrano, A., Martinez, A.T., Guallar, V., Alcalde, M., 2019. Structure-guided evolution of aryl alcohol oxidase from pleurotus eryngii for the selective oxidation of secondary benzyl alcohols. Adv. Synth. Catal. 361, 2514–2525.
Vinod, C.P., Wilson, K., Lee, A.F., 2011. Recent advances in the heterogeneously catalysed aerobic selective oxidation of alcohols. J. Chem. Technol. Biot. 86, 161–171.
Wang, Q., Chen, L.F., Guan, S.L., Zhang, X., Wang, B., Cao, X.Z., Yu, Z., He, Y.F., Evans, D.G., Feng, J.T., Li, D.Q., 2018. Ultrathin and vacancy-rich CoAl-layered double hydroxide/graphite oxide catalysts: promotional effect of cobalt vacancies and oxygen vacancies in alcohol oxidation. ACS Catal. 8, 3104–3115.
Wu, G.W., Cao, E.H., Ellis, P., Constantinou, A., Kuhn, S., Gavriilidis, A., 2019b. Continuous flow aerobic oxidation of benzyl alcohol on Ru/Al_2O_3 catalyst in a flat membrane microchannel reactor: an experimental and modelling study. Chem. Eng. Sci. 201, 386–396.
Wu, G.W., Cao, E.H., Ellis, P., Constantinou, A., Kuhn, S., Gavriilidis, A., 2019. Development of a flat membrane microchannel packed-bed reactor for scalable aerobic oxidation of benzyl alcohol in flow. Chem. Eng. J. 377.
Wu, H.S., Wang, C.S., 2003. Liquid-solid-liquid phase-transfer catalysis in sequential phosphazene reaction: kinetic investigation and reactor design. Chem. Eng. Sci. 58, 3523–3534.
Xiao, C.L., Zhang, L., Hao, H.C., Wang, W.Z., 2019. High selective oxidation of benzyl alcohol to benzylaldehyde and benzoic acid with surface oxygen vacancies on $W_{18}O_9$/holey ultrathin g-C_3N_4nanosheets. ACS Sustain. Chem. Eng. 7, 7268–7276.
Xu, F., 1996. Oxidation of phenols, anilines, and benzenethiols by fungal laccases: Correlation between activity and redox potentials as well as halide inhibition. Chem. Rev. 23, 7608–7614.
Yadav, G.D., Krishnan, M.S., 1999. Solid acid catalysed acylation of 2-methoxy-naphthalene: role of intraparticle diffusional resistance. Chem. Eng. Sci. 54, 4189–4197.
Yang, X.Y., Wu, S.J., Hu, J., Fu, X.R., Peng, L., Kan, Q.B., Huo, Q.S., Guan, J.Q., 2016. Highly efficient N-doped magnetic cobalt-graphene composite for selective oxidation of benzyl alcohol. Catal. Commun. 87, 90–93.
Zeng, Z., Wen, M.F., Yu, B.X., Ye, G., Huo, X.M., Lu, Y.X., Chen, J., 2018. Polydopamine induced in-situ formation of metallic nanoparticles in confined microchannels of porous membrane as flexible catalytic reactor. ACS Appl. Mater. Interfances 10, 14735–14743.
Zhang, Y., Cui, X.J., Shi, F., Deng, Y.Q., 2012. Nano-gold catalysis in fine chemical synthesis. Chem. Rev. 112, 2467–2505.
Zhang, S.Z., Zhu, C.Y., Feng, H.S., Fu, T.T., Ma, Y.G., 2021. Intensification of gas-liquid two-phase flow and mass transfer in microchannels by sudden expansions. Chem. Eng. Sci. 229.
Zhang, W., Oulego, P., Sharma, S.K., Yang, X.L., Li, L.J., Rothenberg, G., Shiju, R., 2020. Self-exfoliated synthesis of transition metal phosphate nanolayers for selective aerobic oxidation of ethyl lactate to ethyl pyruvate. ACS Catal. 10, 3958–3967.
Zhao, S.F., Wang, W.T., Shao, T., Zhang, M.X., Jin, Y., Cheng, Y., 2013. Mixing performance and drug nano-particle preparation inside slugs in a gas-liquid microchannel reactor. Chem. Eng. Sci. 100, 456–463.
Zhao, S.N., Yao, C.Q., Dong, Z.Y., Liu, Y.Y., Chen, G.W., Yuan, Q., 2018. Intensification of liquid-liquid two-phase mass transfer by oscillating bubbles in ultrasonic microreactor. Chem. Eng. Sci. 186, 122–134.
Zhou, X.T., Ji, H.B., 2010. Biomimetic kinetics and mechanism of cyclohexene epoxidation catalyzed by metalloporphyrins. Chem. Eng. J. 156, 411–417.
Zhou, X.T., Chen, H.Y., Han, Q., Lv, M., Ji, H.B., 2020. Acetylacetone as an oxygen activator to improve efficiency for aerobic oxidation of toluene and its derivatives by using cobalt *meso*-tetraphenylporphyrin. New J. Chem. 44, 10286–10291.
Zhou, X.T., Ji, H.B., 2012. Cobalt porphyrin immobilized on montmorillonite: ahighly efficient and reusable catalyst for aerobic oxidation of alcohols to carbonyl compounds. Chin. J. Catal. 33, 1906–1912.